Available online at www.sciencedirect.com
ScienceDirect
Journal of Power Sources 166 (2007) 80–86
JOURNAL OF POWER SOURCES
www.elsevier.com/locate/jpowsour

Short communication

Electrodeposition of nickel nanoparticles on functional MWCNT surfaces for ethanol oxidation

Guan-Ping Jin *, Yan-Feng Ding, Pei-Pei Zheng

Department of Application Chemistry of School of Chemical Engineering, Hefei University of Technology, Hefei 230009, PR China

Received 26 October 2006; received in revised form 14 December 2006; accepted 14 December 2006
Available online 17 January 2007

Abstract

Nickel (Ni) always accumulates on multi-walled carbon nanotubes (MWCNT) by direct electrodeposition. In this paper, nickel nanoparticles were electro crystallized on 4-nitroaniline (NA) radical monolayer-grafted on MWCNT through molecular level design. The structure and nature of the Ni/NA/MWCNT were characterized by field emission scanning electron microscope (FE-SEM), X-ray diffraction (XRD) and X-ray photoelectron spectroscopy (XPS), the results show that Ni nanoparticles were homogeneously electrodeposited on the surfaces of MWCNT. This complex catalyst showed excellent electro-catalytic activity for oxidation of ethanol in alkaline solution.

Keywords: Nano-nickel; Electrodeposition; Characterization; Ethanol oxidation

1. Introduction

Nickel is an effective and cheap catalyst for oxidation of small organic compounds including glucose and glycine [1], carbohydrates [2,3], especially, methanol [4–7] and ethanol [8–13]. For example, nickel redox centers, $Ni(OH)_2$/NiOOH, formed on the nickel surface show high catalytic activity towards the oxidation of ethanol in alkaline media which possibly undergo competition between $2e^-$ to the aldehyde and $4e^-$ to carboxylic acid [2,3,14–17].

On the other hand, MWCNT is an outstanding catalyst support due to its excellent mechanical characteristics, nanometer size and high surface area [18,19], therefore a MWCNT and Ni composite (Ni/MWCNT) are expected to be a promising new catalyst material. Some studies had revealed various innovative functions, such as protection against corrosion [20,21], enhanced hardness [22], alloying [23] and catalytic performance [24,25]. The Ni/MWCNT can be produced by electro deposition [20–22,24], electroless deposition [23] or pyrolysis [25]. Among these, electro-synthesis could be a better method due to its convenience and economy. But, the Ni nanoparticles often are spontaneously form at the defects of the MWCNT resulting in a gathering effect, further decreasing the innovative functionality. Meanwhile, the Ni density is much larger than the carbon nanotubes, so the control of the interface between the filler and the support has not yet been developed well. Therefore, it is important to make a homogeneously electrodeposited Ni/MWCNT composite.

In this study, a novel method is described for the preparation of nanoparticles of Ni on MWCNT through a molecular level approach for ethanol oxidation.

2. Experimental

2.1. Chemicals

MWCNT with diameters of 10–30 nm and lengths of 1–10 μm were purchased from Sun Nanotech. Co. Ltd. of China and were synthesized by catalytic decomposition of CH_4 on a NiMgO catalyst [26]. All chemicals were of the highest quality that are commercially available: 4-nitroaniline (NA), nickel nitrate ($NiNO_3$), lithium nitrate ($LiNO_3$), choline ($HOCH_2CH_2N^+(CH_3)_3$, Ch), and ethanol (Chemical Regent Factory of Shanghai, China); tetrabutylammonium tetrafluoroborate (n-Bu_4NBF_4) (Fluka). Acetonitrile (ACN) was distilled twice prior to use. All other chemicals were of reagent grade. Doubly distilled water (prepared in a quartz apparatus) was

* Corresponding author. Tel.: +86 551 2902450; fax: +86 551 2902450.
E-mail address: jgp@hfut.edu.cn (G.-P. Jin).

0378-7753/$ – see front matter © 2007 Elsevier B.V. All rights reserved.
doi:10.1016/j.jpowsour.2006.12.087

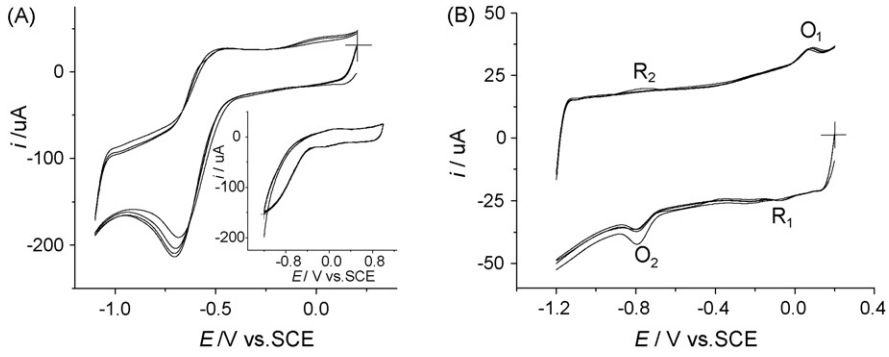

Fig. 1. (A) CVs of a MWCNT electrode derivatized by 4-nitrobenzene radicals from the reduction of 4-nitroaniline in $CH_3CN + 0.1\,M$ n-Bu_4NBF_4. (Inset) MWNCT/Ch/WGE in blank $CH_3CN + 0.1\,M$ n-Bu_4NBF_4. (B) CVs of a MWCNT electrode derivatized by 4-aminobenzene radicals from the reduction of 4-nitrobenzene radicals in 90:10 $H_2O + C_2H_5OH + 0.1\,M$ KCl. Scan rate: $50\,mV\,s^{-1}$.

used in all experiments. High purity nitrogen gas was used for deaeration.

2.2. Instrumentation

Electrochemical measurements were performed with a model CHI 660 B electrochemical analyzer (Cheng-Hua, Shanghai, China). A conventional three-electrode electrochemical system was used for all electrochemical experiments. The working electrode was a paraffin-impregnated graphite electrode (WGE) with geometric area of $0.125\,cm^{-2}$. A saturated calomel electrode (SCE, KCl) and a platinum electrode were used as the reference and the auxiliary electrode, respectively. Field emission scanning electron microscope (FE-SEM) images were obtained on a JSM-600 field emission scanning electron microanalyser (JEOL, Japan). XPS spectra were recorded by using an ESCALAB MK_2 spectrometer (Vg corporation, UK) with a Mg-Alpha X-ray radiation as the source for excitation. X-ray diffraction (XRD) data of the samples were collected using a Rigaku D/MAX-rB diffractometer with Cu Kα radiation.

2.3. Preparation of electrodes

The 10 mg MWCNT were dispersed in 10 ml of mixed acid solution of nitric acid and perchlorate acid (7:3). The mixed solution was ultrasonically agitated for 7 h. The MWCNT were washed with doubly distilled water to a neutral pH, then washed with acetone and dried in air. The peaks at 1735 and $1590\,cm^{-1}$ in the FTIR spectrum suggested that carboxylic acid groups and carboxylate groups were present on the surface of the MWCNT [27]. About 2.5 mg of mixed acid-treated MWCNT was dispersed in 10 ml of acetone with the aid of ultrasonic agitation to give $0.25\,mg\,ml^{-1}$ black suspension.

The WGE electrode was step by step polished to a mirror-like finish with fine wet emery paper (grain size 1000, 3000, 4000), followed by sonication in ethanol and water for 15 min, respectively. After cleaning, the choline modified WGE (Ch/WGE) with a positive charge was fabricated using the anode oxidation method by C–O bond in order to bond MWCNT with charge [28]. Some microliters of the mixed acid-treated MWCNT solution were cast onto the surface of Ch/WGE, and the solvent acetone was evaporated, after rinsing with distilled water, the electrode was termed: MWCNT/Ch/WGE [29].

The electro-synthesis of Ni nanoparticles on the MWCNT surface followed the literature [30] process. Firstly, the MWCNT/Ch/WGE electrode was immersed into a solution including $CH_3CN + 0.1\,M$ n-$Bu_4NBF_4 + 5.0\,mM$ 4-nitroaniline (NA), modified by 4-nitrobenzene radicals via a –C–C– bond using the cyclic voltammetry method (CV). After rinsing with distilled water, the electrode was transferred into a protonic solution including 90:10 $H_2O + C_2H_5OH + 0.1\,M$ KCl, then, the NO_2 group in 4-nitrobenzene on the electrode surface was reduced to the NH_2 group by applying a potential of $-1.2\,V$ for 600 s; secondly, the 4-aminobenzene monolayer-grafted MWCNT electrode (NA/MWCNT/Ch/WGE) was then immersed into a solution including $0.018\,M$ $NiNO_3 + CH_3CN + 0.01\,M$ KNO_3 for 20 min; Thirdly, after rinsing thoroughly with $CH_3CN/0.01\,M$ KNO_3 solution, the Ni^{2+} adsorbed NA/MWCNT/Ch/WGE electrode was transferred into $CH_3CN/0.01\,M$ KNO_3 solution, Ni nanoparticles were grown on NA/MWCNT/Ch/WGE by CV method, and recorded as Ni/NA/MWCNT/Ch/WGE.

3. Results and discussion

3.1. Preparation of a 4-nitrobenzene radical monolayer on MWCNT/Ch/WGE surface

Fig. 1(A) shows the CVs of MWCNT/Ch/WGE in the presence and absence (inset) of 5.0 mM 4-nitroaniline in $CH_3CN/0.1\,M$ n-Bu_4NBF_4 solution. In both states, a pair of redox peaks (0.1/0.0 V) can be seen matching oxygen function of MWCNT [31]. In the presence of 4-nitroaniline, there is another irreversible reduction peak at $-0.70\,V$ decreasing with repeated scanning. This indicates the formation of a diazonium derivative corresponding to reaction (***) in Scheme 1 [32], which can further produce 4-nitrobenzene radicals linking with the MWCNT by a –C–C– bond [30,33–36]. Fig. 1(B) shows the transformation of NO_2 groups into NH_2 in the protonic solution (90:10 $H_2O + C_2H_5OH + 0.1\,M$ KCl). There is an irreversible reduction peak at $-0.79\,V$ gradually diminishing on continuous cycling with a small oxidation peak at

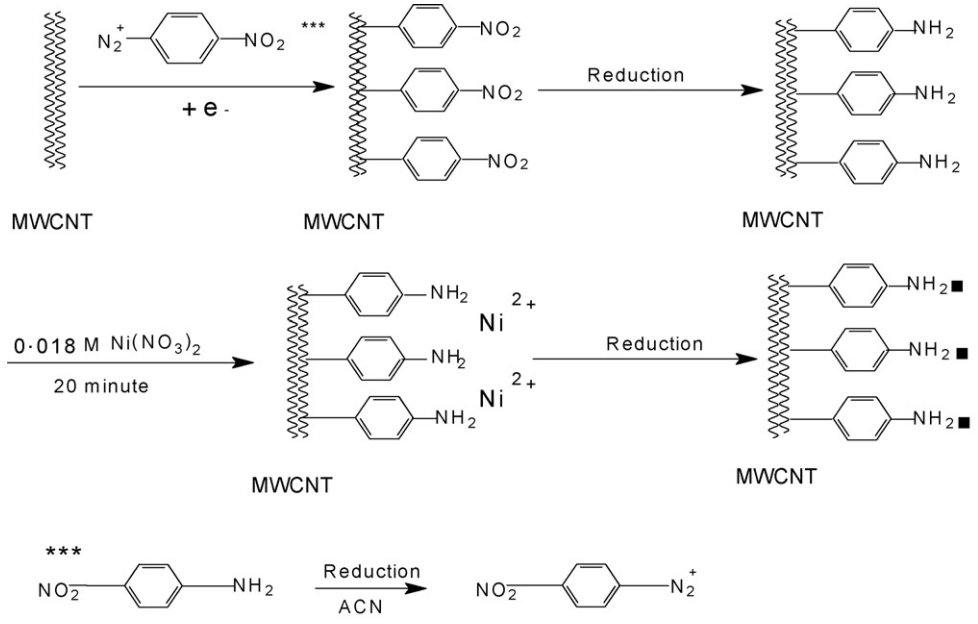

Scheme 1.

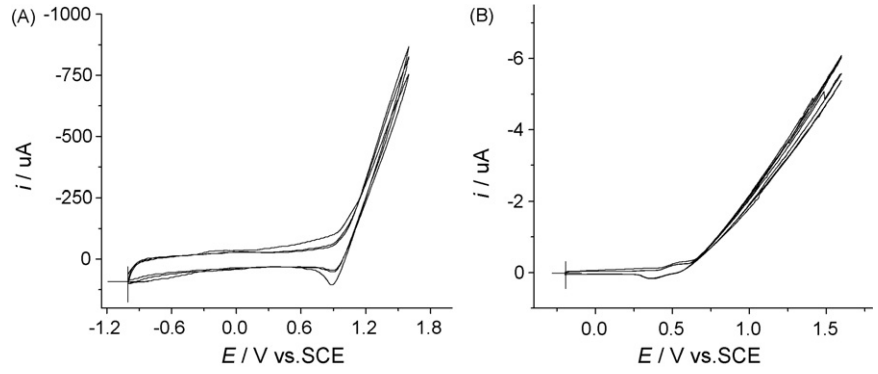

Fig. 2. (A): Reduction of Ni^{2+} at NA/MWCNT/Ch/WGE; medium: 0.01 M KNO_3/ACN. (B) The transformation of Ni at NA/MWCNT/Ch/WGE in 0.1 M NaOH. Scan rate: 20 mV s^{-1}.

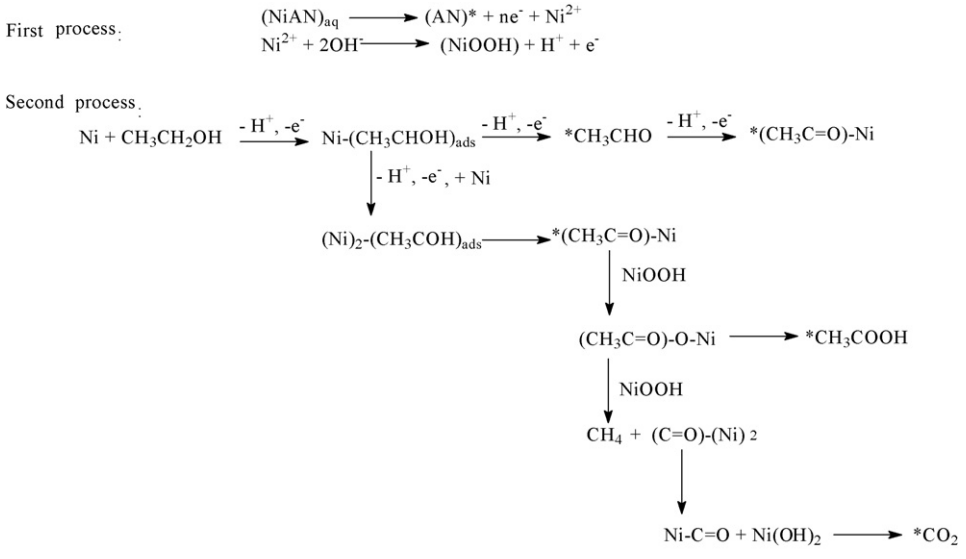

Scheme 2.

−0.77 V, it suggests a gradual reduction of NO_2 to NH_2 within the grafted layer [30,36]. This suggests Scheme 1. The quantity of NH_2 on the MWCNT/Ch/WGE surface is estimated from the charge in the first scan, calculated by integration of the first cathode peak [28,30]. The concentration of Ni in Fig. 1(B) is 1.6×10^{-10} mol cm^{-2}. This electrode was termed: NA/MWCNT/Ch/WGE.

3.2. Preparation of Ni nanoparticles on the NA/MWCNT/Ch/WGE surface

After grafting the 4-aminobenzene monolayer, the NA/MWCNT/Ch/WGE was immersed in a 0.018 M $Ni(NO_3)_2$/0.01 M KNO_3/ACN solution for 20 min then rinsed thoroughly with a blank solution. The Ni^{2+} modified NA/MWCNT/Ch/WGE was then placed in a blank ACN/0.01 M KNO_3 solution, then, electrodeposited by the CV method until the reduction peak stopping declining Fig. 2(A) shows an irreversible reduction peak at 0.80 V corresponding to the growth of Ni nanoparticles on NA/MWCNT/Ch/WGE. Fig. 2(B) displays the transformation of Ni to NiOOH and $Ni(OH)_2$ at 0.52–0.36 V matching Scheme 2 [14–17]. The anodic peak currents are linearly proportional to the scan rate up to 400 mV s^{-1}, suggesting an adsorption-controlled process. The quantity of Ni deposition is estimated from the charge, calculated by integration of the anodic peak. The concentration in Fig. 2(B) is 2.5×10^{-10} mol cm^{-2}.

3.3. FE-SEM of Ni electrodeposits at NA/MWCNT/Ch/WGE

Fig. 3 shows a FE-SEM micrograph of the Ni electrodeposits for the MWCNT/Ch/WGE (A) and NA/MWCNTs/Ch/WGE (B) in 0.01 M KNO_3/ACN. As shown in Fig. 3(A) and the inset,

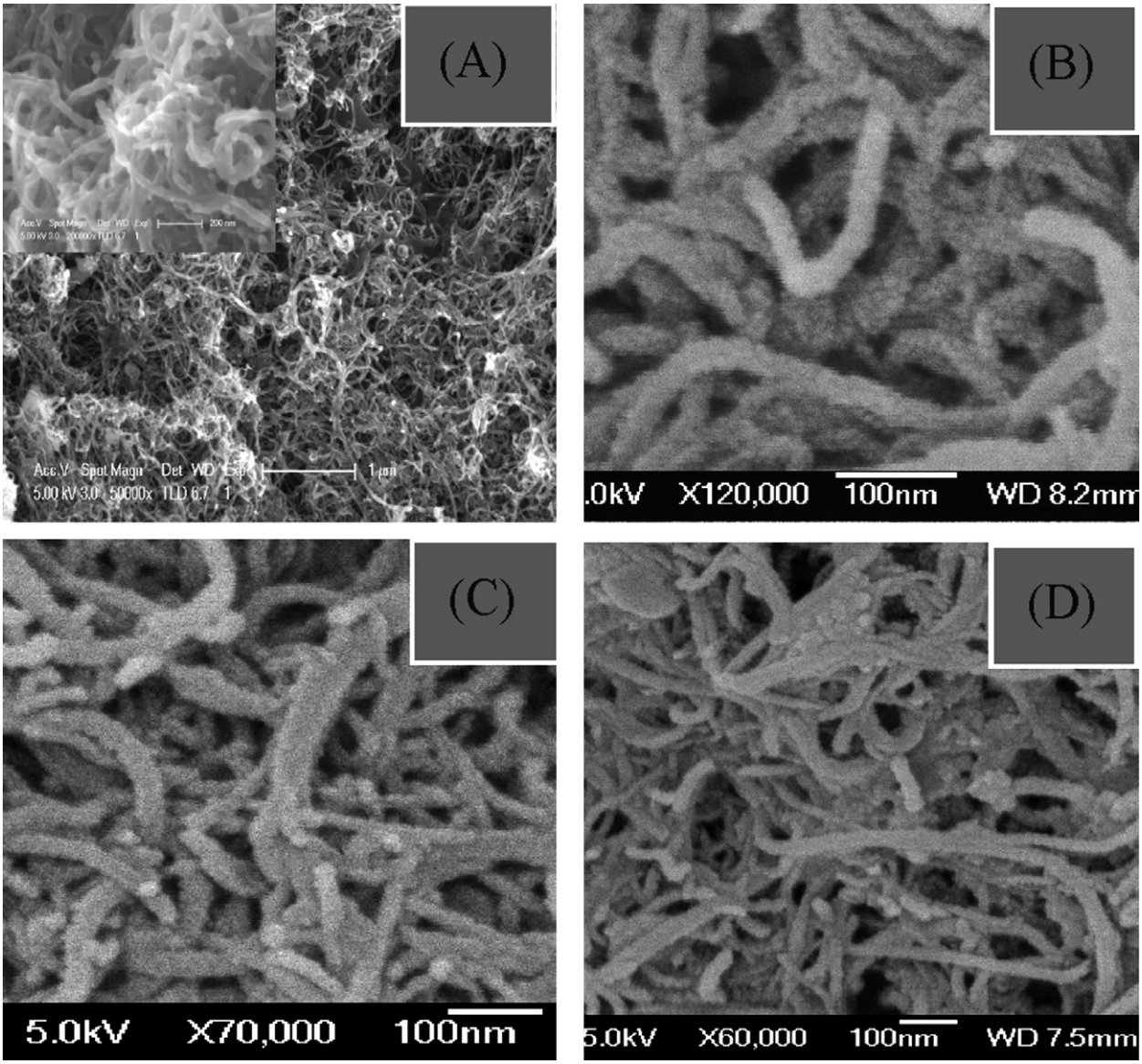

Fig. 3. FE-SEM of Ni electrodeposits at MWCNT/Ch/WGE (A) and inset for 20 min, at NA/MWCNT/Ch/WGE for 20 min (B), 40 min (C) and 80 min (D); medium: 0.01 M KNO_3/ACN.

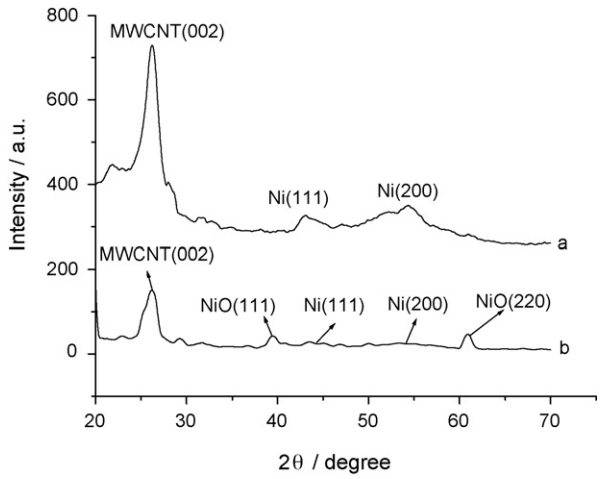

Fig. 4. X-ray diffraction (XRD) pattern of Ni/NA/MWCNT (a) and Ni/MWCNT (b) composites.

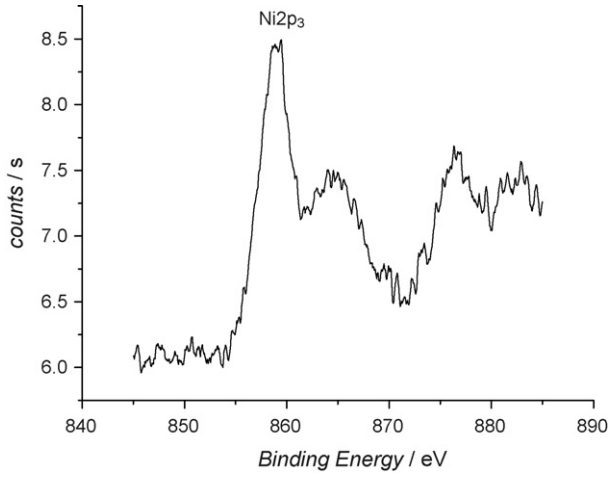

Fig. 5. XPS of Ni/NA/MWCNT/Ch/WGE prepared in 0.1 M NaOH.

because the carboxylic acid groups on the surface of MWCNT can stimulate the deposition of Ni. The Ni nanoparticles spontaneously formed at the local defects and end of MWCNT with a lot of irregular aggregate islands [37]. However, Fig. 3(B) shows a homogeneous electrodeposition effect of Ni nanoparticles on the surface of NA/MWCNT/Ch/WGE with about 8 nm in diameter. The reasons can be as follows: the 4-aminobenzene group modified on the MWCNT surface by C–C covalent bonds is an excellent substrate for Ni nanoparticle deposition. The 4-aminobenzene monolayer on the MWCNT surface provides a uniform functional surface, which can effectively prevent the preferred nucleation process on the MWCNT surface. Therefore, the present results demonstrate the possibility to control the morphology of Ni-deposition with minimal surface deactivation.

Moreover, the density of the Ni deposition depends on the immersion time and concentration of the nickel nitrate. As can be seen in Fig. 3(C) and (D), the Ni nanoparticles are gradually overlapping with time increasing from 40 to 80 min, compared with that in Fig. 3(B), therefore, the optimum immersion time should be 20 min. While the concentration of nickel nitrate is more than 0.1 M with immersion time in 20 min, the deposition occurs overlapping.

3.4. XRD analysis of Ni/NA/MWCNT composites

Fig. 4 shows that XRD pattern of Ni/NA/MWCNT (a) and Ni/MWCNT (b) composites. There is a typical reflection peak (0 0 2) in MWCNT or graphite at 21.8° in two curves [37]. The diffraction peaks in Ni/MWCNT (b) display a mixture effect of NiO and Ni nanoparticles, the peaks at 37.3°, 43.3° and 63.0° correspond to characteristic peaks of rock salt structured NiO, which can be assigned to (1 1 1), (2 0 0) and (2 2 0) (2θ) reflection of fcc phase NiO [38,39], also observed, are two small diffraction peaks at 44° and 52° matching Ni (1 1 1) and (2 0 0) [40]. The size of the NiO and Ni nanoparticles are respectively about 1.05 μm and 6.6 nm calculated using the Scherrer formula. However, the XRD patterns of the Ni/NA/MWCNT (a) composites only exhibit the characteristic peaks of Ni at 44° and 52° (2θ) with an average size of 7.2 nm. This illustrates that the MWCNT modified by 4-aminobenzene can not only effectively avoid the preferred nucleation process on the MWCNT surface, but also control the nanoparticle size. This result is significant in the synthesizing of metal catalyst with a MWCNT support.

3.5. XPS characterization of Ni/NA/MWCNT composites

X-ray photoelectron spectroscopy was used to probe the chemical nature and oxidation state of the Ni/NA/MWCNT composites transformed in 0.1 M NaOH. The Ni $2p_{3/2}$, O 1s and C 1s regions were analysed for each specimen. Typical XPS spectra of Ni 2p3/2 are shown in Fig. 5, which gives two different nickel oxide species at 855.9 ± 0.3 and 857.9 ± 0.3 eV of binding energy assigned to $Ni(OH)_2$ and NiOOH species [4,11], respectively. This result agrees with Scheme 2. This ver-

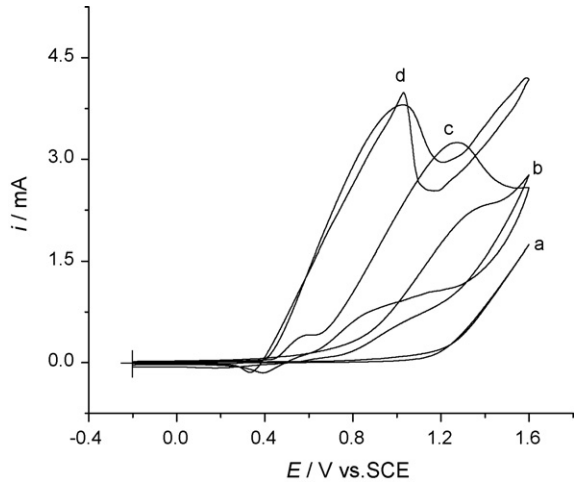

Fig. 6. CVs of 0.03 M C_2H_5OH at WGE (a), MWCNT/Ch/WGE (b), Ni/MWCNT/Ch/WGE (c) and Ni/NA/MWCNT/Ch/WGE (d) in 0.1 M NaOH. Scan: 100 mV s^{-1}.

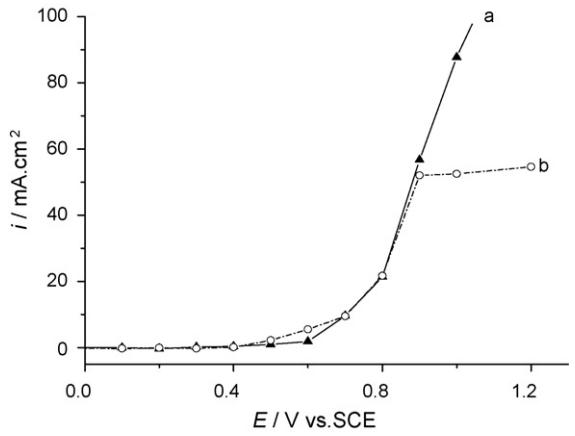

Fig. 7. The steady-state polarisation curves of Ni/NA/MWCNT/Ch/WGE (a) and Ni/MWCNT/Ch/WGE (b) in 3.43 M C_2H_5OH + 0.1 M NaOH.

ifies the transformation of Ni to NiOOH and $Ni(OH)_2$ in 0.1 M NaOH.

3.6. Electrocatalytic oxidation of ethanol at Ni/NA/MWCNT/Ch/WGE

Fig. 6 shows the CVs of 0.03 M C_2H_5OH at WGE (a), MWCNT/Ch/WGE (b), Ni/MWCNT/Ch/WGE (c) and Ni/NA/MWCNT/Ch/WGE (d) in 0.1 M NaOH. It can be readily seen that the Ni/NA/MWCNT/Ch/WGE shows an excellent electrocatalytic oxidation of C_2H_5OH compared with the other modified electrodes with a sharply increasing peak current and negative potential. The oxidation of ethanol undergoes two processes, one corresponds to the formation of Ni(III) species with a reversible transformation of $Ni(OH)_2$/NiOOH on Ni/NA/MWCNT/Ch/WGE, and ultimately NiO/NA/MWCNT/Ch/WGE is shaped [14–17]. The other is only Ni(III) species (NiOOH) produced at the electrode surface, in the presence of ethanol a new anodic peak with a large peak current is formed (d). This suggests that ethanol is oxidized and accompanied by the transformation of NiOOH to $Ni(OH)_2$ [4,13,41]. Therefore, NiOOH probably acts as an electro catalyst [8]. On the basis of the above literature, we propose the following mechanism 2 for the mediated electrooxidation of ethanol on Ni/NA/MWCNT/Ch/WGE electrode.

3.7. The steady-state polarisation curves of Ni/MWCNT/Ch/WGE and Ni/NA/MWCNT/Ch/WGE

Fig. 7 shows steady-state polarisation curves of Ni/NA/MWCNT/Ch/WGE (a) and Ni/MWCNT/Ch/WGE (b) in 3.43 M C_2H_5OH + 0.1 M NaOH. The two catalysts displayed a similar effect for the oxidation of ethanol at a lower potential (<0.9 V), however, the activity of the Ni/NA/MWCNT increases considerably compared with that of the Ni/MWCNT with a rising response in higher potentials (>0.9 V). The reason is probably the homogeneously electrodeposited Ni nanoparticles on the surfaces of NA/MWCNT/Ch with a larger area and a smaller size. This result is consistent with Fig. 6.

4. Conclusion

A novel method for preparing homogeneously electrodeposited Ni nanoparticles is proposed on the surfaces of MWCNT. In situ FE-SEM reveals that the homogeneous, spherical nanoparticles are anchored on the external walls of MWCNT. The average size of these particles was 7.2 nm. Preliminary tests indicated that the Ni/NA/MWCNT composite exhibits a high catalytic activity for the electrooxidation of ethanol. This simple nanoparticle deposition technique is not limited to Ni but may be used to prepare a variety of metallic nanoparticles on MWCNT surfaces for application as catalysts in fuel cells.

Acknowledgements

The authors gratefully acknowledge financial support from Science Research Program Fund of Hefei City, and Doctor Fund of Hefei University of Technology.

References

[1] I.H. Yeo, D.C. Johnson, J. Electroanal. Chem. 495 (2001) 110–119.
[2] T.R.I. Cataldi, E. Desimoni, G. Ricciardi, F. Lelj, Electroanalysis 7 (1995) 435–442.
[3] T.R.I. Cataldi, D. Centoze, G. Ricciardi, Electroanalysis 7 (1995) 305–312.
[4] A.N. Golikand, M. Asgari, M.G. Maragheh, S. Shahrokhian, J. Electroanal. Chem. 588 (2006) 155–160.
[5] A. Ciszewski, G. Milczarek, J. Electroanal. Chem. 426 (1997) 125–130.
[6] I.G. Casella, T.R.I. Cataldi, A.M. Salvi, E. Desimoni, Anal. Chem. 65 (1993) 3143–3150.
[7] A.A. El-Shafei, J. Electroanal. Chem. 471 (1999) 89–95.
[8] M. Fleischmann, K. Korinek, D. Pletcher, J. Chem. Soc, Perkin Trans. 2 (1972) 1396.
[9] Y.C. Weng, J.F. Rick, T.C. Chou, Biosensors Bioelectron. 20 (2004) 41–51.
[10] G.C. Fiaccabrino, M. Koudelka-Hep, Electroanalysis 10 (1998) 217–222.
[11] E.T. Hayes, B.K. Bellingham, H.B. Mark, A. Galal, Electrochim. Acta 41 (1996) 337–344.
[12] Y.Y. Liao, T.C. Chou, Electroanalysis 12 (2000) 55–59.
[13] S. Berchmans, H. Gomathi, G.P. Rao, J. Electroanal. Chem. 394 (1995) 267–270.
[14] P.V. Samant, J.B. Fernandes, J. Power Sources 79 (1999) 114–118.
[15] R.S. Schebler-Guzam, J.R. Vielche, A. Arvia, J. Electrochem. Soc. 125 (1978) 1578–1582.
[16] R.S. Schebler-Guzam, J.R. Vielche, A. Arvia, Corros. Sci. 18 (1978) 441–449.
[17] A. Seghioure, J. Chevalet, A. Barboun, F. Lantelme, J. Electroanal. Chem. 442 (1998) 113–123.
[18] L.J. Sheli, Nature 354 (1991) 56–58.
[19] S. Iijima, T. Ichihashi, Nature 363 (1993) 603–605.
[20] X.H. Chen, F.Q. Cheng, S.L. Li, L.P. Zhou, D.Y. Li, Surf. Coat. Technol. 155 (2002) 274–278.
[21] X.H. Chen, C.S. Chen, H.N. Xiao, F.Q. Cheng, G. Zhang, G.J. Yi, Surf. Coat. Technol. 191 (2005) 351–356.
[22] S. Arai, M. Endo, N. Kaneko, Carbon 42 (2004) 641–644.
[23] A. Misra, P.K. Tyagi, M.K. Singh, D.S. Misra, J. Ghatak, P.V. Satyam, D.K. Avasthi, Diamond Related Mater. 15 (2006) 300–303.
[24] F. Wang, S. Arai, M. Endo, Carbon 43 (2005) 1716–1721.
[25] P.D. Kichambare, D. Qian, E.C. Dickey, C.A. Grimes, Carbon 40 (2002) 1903–1909.
[26] P. Chen, H.B. Zhang, G.D. Lin, Q. Hong, K.R. Tasai, Carbon 35 (1997) 1051–1495.
[27] P.X. Hou, S. Bai, Q.H. Yang, C. Liu, H.M. Cheng, Carbon 40 (2002) 81–85.
[28] G.P. Jin, X.Q. Lin, Electrochem. Commun. 6 (2004) 454–460.

[29] G.P. Jin, J.B. He, Z.B. Rui, F.S. Meng, Electrochimica Acta 51 (2006) 4341–4346.
[30] Z. Tang, S. Liu, S. Dong, E. Wang, J. Electroanal. Chem. 502 (2001) 146–151.
[31] F.H. Wu, G.C. Zhao, X.W. Wei, Electrochem. Commun. 4 (2002) 690–694.
[32] L.S. Wang, F.L. Tang, J.R. Lu, Organic Chemistry, Publish Company of Dong Nang University, p. 322.
[33] M. Delamar, R. Hitmi, J. Pison, J.M. Saveant, J. Am. Chem. Soc. 114 (1992) 5883–5884.
[34] H. Yang, R.L. McCreery, Anal. Chem. 71 (1999) 4081–4087.
[35] C. Bourdillon, M. Delamar, C. Demaille, R. Hithi, J. Moiroux, J. Pinson, J. Electroanal. Chem. 336 (1992) 113–123.
[36] P. Allongue, M. Delamar, B. Desbat, O. Fagebaume, R. Hitmi, J. Pison, J.M. Saveant, J. Am. Chem. Soc. 119 (1997) 201–207.
[37] D.J. Guo, H.L. Li, Carbon 43 (2005) 1259–1264.
[38] F.B. Zhang, Y.K. Zhou, H.L. Li, Mater. Chem. Phys. 83 (2004) 260–264.
[39] X.M. Liu, X.G. Zhang, Electrochim. Acta 49 (2004) 229–232.
[40] C.C. Hu, C.Y. Lin, T.C. Wen, Mater. Chem. Phys. 44 (1996) 233–238.
[41] M. Fleischmann, K. Korinek, D. Pletcher, J. Electroanal. Chem. 31 (1971) 39–49.